4-15-2012

Sorption kinetic study of selenite and selenate onto a high and low pressure aged iron oxide nanomaterial

Christina M. Gonzalez

Jeffrey Hernandez

Jose R. Peralta-Videa

Cristian E. Botez

Jason Parsons
The University of Texas Rio Grande Valley, jason.parsons@utrgv.edu

See next page for additional authors

Recommended Citation

Gonzalez CM, Hernandez J, Peralta-Videa JR, Botez CE, Parsons JG, Gardea-Torresdey JL. Sorption kinetic study of selenite and selenate onto a high and low pressure aged iron oxide nanomaterial. J Hazard Mater. 2012;211-212:138-145. doi:10.1016/j.jhazmat.2011.08.023

Published in final edited form as:
J Hazard Mater. 2012 April 15; 0: 138–145. doi:10.1016/j.jhazmat.2011.08.023.

Sorption kinetic study of selenite and selenate onto a high and low pressure aged iron oxide nanomaterial

Christina M. Gonzalez[1], **Jeffrey Hernandez**[1], **Jose R. Peralta-Videa**[1], **Cristian E. Botez**[4], **Jason G. Parsons**[3], and **Jorge L. Gardea-Torresdey**[1,2,*]

[1]Department of Chemistry, The University of Texas at El Paso; 500 W University Ave., El Paso TX 79968, United States

[2]Environmental Science and Engineering PhD program, The University of Texas at El Paso; 500 W University Ave., El Paso TX 79968, United States

[3]Department of Chemistry, The University of Texas-Pan American 1201 W University Drive, Edinburg TX 78534, United States

[4]Department of Physics, The University of Texas at El Paso; 500 W University Ave., El Paso TX 79968, United States

Abstract

The sorption of selenite (SeO_3^{2-}) and selenate (SeO_4^{2-}) onto Fe_3O_4 nanomaterials produced by non microwave-assisted or microwave-assisted synthetic techniques was investigated through use of the batch technique. The phase of both synthetic nanomaterials was determined to be magnetite by X-ray diffraction. The average grain sizes of non microwave-assisted and microwave-assisted synthetic Fe_3O_4 were determined to be 27 and 25 nm, respectively through use of the Scherrer's equation. Sorption of selenite was pH independent in the pH range of 2-6, while sorption of selenate decreased at pH 5 and 6. The addition of Cl^- had no significant effect on selenite or selenate binding, while the addition of NO_3^- only affected selenate binding to the microwave assisted Fe_3O_4. A decrease of selenate binding to both synthetic particles was observed after the addition of SO_4^{2-} while selenite binding was not affected. The addition of PO_4^{3-} beginning at concentrations of 0.1 ppm had the most prominent effect on the binding of both selenite and selenate. The capacities of binding, determined through the use of Langmuir isotherm, were found to be 1923 and 1428 mg Se/kg of non microwave-assisted Fe_3O_4 and 2380 and 2369 mg Se/kg of microwave-assisted Fe_3O_4 for selenite and selenate, respectively.

Keywords

Selenite; Selenate; magnetite; adsorption; DRC-ICP-MS

*Corresponding Author: phone (915)747-5359, Fax (915)747-5847, jgardea@utep.edu.

1. Introduction

The narrow range between selenium deficiency and toxicity in humans is of concern today. Deficiency occurs when daily consumption is less than 0.1 mg Se/kg of body weight, while toxicity occurs when consumption per day is above 1 mg Se/kg of body weight [1]. As drinking water is a primary source in which selenium can enter the human body, the U. S. Environmental Protection Agency has set the maximum contaminant level in drinking water to be 0.05 mg Se/L, [2-3]. Wild animals are also at risk when high concentrations of selenium are present in water systems. It has been reported that in waterfowl, high levels of selenium are embryotoxic and teratogenic [4]. In water, selenium exists predominately as the inorganic forms selenite (SeO_3^{2-}, where the Se is present as the Se^{4+} ion) and selenate (SeO_4^{2-}, where the Se is present as the Se^{6+} ion) [5].

There has been a variety of treatment technologies developed for the remediation of both selenium oxoanions in water including bacterial reduction, membrane filtration, chemical reduction, reverse osmosis, and solar ponds [6-8]. However, these treatment technologies are not cost effective. An alternative treatment technique that has been gaining increasing attention in study over the past decade is adsorption. Adsorbents such as sulphuric acid-treated peanut shell, hydrocalumite, ettringite, $AlPO_4$, biopolymeric materials, aluminum-based water treatment residuals, hardened cement paste, cement minerals, aluminum oxides, iron oxyhydroxides, iron coated sand, and zero valent iron have been tested for the removal of selenium [8-17]. The use of magnetic materials as adsorbents may emerge as an even more efficient form of treatment technology. Magnetic materials are promising materials for adsorption because they can easily be removed from aqueous effluents by a simple process known as magnetic separation [18]. These materials are also useful because they produce no further contaminants such as flocculants and are capable of treating large amount of wastewater within a short amount of time [19].

The iron oxide magnetite (Fe_3O_4) is an adsorbent with magnetic properties. A study by Martinez *et al.* [20] has shown that a naturally occurring magnetite with a particle size <5 μm has been capable of binding selenite and selenate at acidic pH. Lopez de Arroyabe Loyo *et al.* [21] reported rapid selenite binding to ultra small Fe_3O_4 and Fe/Fe_3C particles, but did not test the capacity of the material nor its ability for selenate adsorption. These studies indicate that magnetite may be a promising adsorbent for selenium removal. However, many previous studies for selenium oxoanion removal do not investigate the ability of the adsorbent to remove both selenite and selenate. Also, the effects of naturally occurring potential competitive anions Cl^-, NO_3^-, SO_4^{2-}, or PO_4^{3-} on selenium oxoanion removal have not been thoroughly investigated.

In this research, the magnetic iron oxide Fe_3O_4 was synthesized by both non microwave-assisted and microwave-assisted synthetic techniques. The nanomaterials produced by both of these techniques were determined to have the crystal structure of magnetite. The Fe_3O_4 nanomaterials' adsorption capacities for selenite and selenate were tested in the pH range of 2 through 6 and as a function of time. The effects of the addition of individual competitive anions Cl^-, NO_3^-, SO_4^{2-}, or PO_4^{3-} added to solution in a range of 0.1 to 100 ppm were also investigated. Finally, the capacities of both synthetic nanomaterials for selenite or selenate

binding were studied using selenium concentrations of 0.25 through 10 ppm and fitted with Langmuir isotherms.

2. Methodology

2.1. Solution preparation

Reagent grade Na_2SeO_3 (Aldrich), Na_2SeO_4 (Alfa Aesar), NaCl (Aldrich), $Mg(NO_3)_2{\cdot}6H_2O$ (Mallinckrodt), K_2SO_4 (J.T. Backer), and $Na_3PO_4{\cdot}12H_2O$ (EM Science) chemicals were dissolved in Millipore (18 mΩ) water to obtain stock solutions of selenite, selenate, chloride, nitrate, sulfate and phosphate, respectively. The prepared stock solutions were diluted to proper concentrations for the following research experiments.

2.2. Synthesis of the iron oxide nanomaterial

For the synthesis of the iron oxide nanomaterials, two separate 1.0 L solutions of 30 mM Fe(II) (from $FeCl_2$, EM Science) were prepared. Both solutions were slowly titrated separately for 1 h with 90 mL of 1.0 M NaOH solution (from NaOH, VWR International West Chester, Pennsylvania) to obtain a ratio of 1:3 ratio of Fe^+:OH^-. The slow rate of titration was to prevent the precipitation of $Fe(OH)_3$. After completion of the titration, one of the two titrated solutions was heated to 90° C for 1 h on a heating plate and resulted in the non microwave-assisted Fe_3O_4 nanomaterial. The other titrated solution was transferred into sealed vessels and placed in a Perkin Elmer Mulitwave 2000 system (Shelton CT, USA). The sealed vessels were heated to a temperature of 90° C and held constant for 25 min at a pressure of 75 bars and resulted in the microwave-assisted Fe_3O_4 nanomaterial. Both sets of prepared nanomaterials were cooled to room temperature and centrifuged at 3000 rpm (Fisher Scientific 8K, Houston, TX) for 5 min after each of the techniques were completed. To remove any byproducts that may have been generated during the synthesis, the nanomaterials were then washed twice with deionized water (DI). Subsequently, the nanomaterials were then dried in a VWR 1305U oven (VWR International, West Chester, PA) at 100° C for 24 h. Lastly, the nanomaterials were homogenized into a powder using a mortar and pestle for both analysis and experimental use.

2.3. XRD characterization

Powder x-ray diffraction (XRD) data were collected from both synthetic nanomaterials using a Siemens D5000 diffractometer (Bruker AXS GmbH, Germany). Samples were placed on a platinum holder and XRD patterns were collected at room temperature in the reflection geometry within a 2θ angular range between 25 and 60°. A step of 0.007° and counting time of 8 s / step were used. Both XRD datasets were first analyzed using the FULLPROF suite of programs and crystallographic data from the literature to determine the phases present in each nanomaterial [22]. Subsequently, Gaussian fits of three diffraction peaks for each XRD pattern were used to determine the average grain size of each nanomaterial via Scherrer's formalism.

2.4. Binding pH profile

In these studies, all experiments were performed at room temperature. The binding of either selenite or selenate to both synthetically prepared Fe_3O_4 nanomaterials were determined

over a pH range of 2 to 6. The pH of the 100 ppb selenite or selenate solutions were adjusted to pH 2, 3, 4, 5, or 6 using dilute hydrochloric acid or sodium hydroxide prior to reactions. The reactions were carried out in 5 mL polyethylene reaction tubes containing 10 mg of either nanomaterial with a 4 mL aliquot of 100 ppb of selenite or selenate at each pH. The reaction tubes were then rocked (Specimix, Thermo Scientific) and allowed to equilibrate for 60 min at room temperature. The samples were than centrifuged at 3000 rpm for 7 min and the resulting supernatants were collected for analysis in dynamic reaction cell-inductively-coupled plasma-mass spectrometer (DRC-ICP-MS) ELAN DRCII (Perkin Elmer, Shelton, CT) to determine the amount of selenium oxoanion removed. In addition, control samples containing only pH adjusted selenite or selenate oxoanions were treated the same as the samples to determine the effects of the methodology and polyethylene reaction tubes had on the selenium oxoanion binding. All experiments in this study were conducted in triplicate for statistical purposes.

2.5. Sorption kinetic study

The time required for either selenite or selenate binding to occur to each of the nanomaterials was determined using 100 ppb of selenite or selenate adjusted to pH 4 and reacted with 10 mg of nanomaterial at time intervals ranging from 5-60 min. The pH of 4 was chosen for these experiments because the nanomaterials are both stable at this pH and there was no significant change in binding above this pH level found in the previous study. The pH adjustment was carried out as described in the pH binding study. A 4 mL aliquot of either 100 ppb selenite or selenate solution was added to 10 mg of either non microwave-assisted or microwave-assisted nanomaterial and was allowed to equilibrate. The binding time intervals investigated were 5, 10, 15, 20, 30, and 60 min. The samples were centrifuged and the supernatant collected for analysis using DRC-ICP-MS.

2.6. Interference studies

The possible competition for active adsorption sites on both synthetic nanomaterials in the presence of varying concentrations of Cl^-, NO_3^-, SO_4^{2-}, or PO_4^{3-} was investigated at pH 4. A 4 mL aliquot containing 100 ppb of selenite or selenate solution and either 0.1, 1, 10, or 100 ppm of the possible interfering ion of Cl^-, NO_3^-, SO_4^{2-}, or PO_4^{3-} was reacted with each synthetic nanomaterial for 1 h. After reaction time was completed, the samples were centrifuged and the supernatant was collected for DRC-ICP-MS analysis.

2.7. Adsorption isotherms

The selenium oxoanion binding capacities of both synthetic Fe_3O_4 nanomaterials was investigated using varying concentrations of selenite or selenate in the range of 0.25 to 10 ppm. For these reactions, a 4 mL aliquot of either selenite or selenate at concentrations of 0.25, 0.5, 1, 5, or 10 ppm adjusted to pH 4 were reacted on a rocker with 10 mg of either synthetic nanomaterial for a period of 15 min; which determined as the amount of time required for the binding of Se oxoanions to the Fe_3O_4 to occur. The reactions were performed in triplicate with control samples as mentioned previously. The samples were centrifuged after the reaction time was completed and the supernatant was collected for analysis by DRC-ICP-MS. The obtained data was then fitted to the Langmuir isotherm

equation shown below, where C_e is the concentration at equilibrium of Se(IV/VI), Q_e is the amount of Se(IV/VI) adsorbed to the nanomaterial at equilibrium, and *Qm* and *b* are constants based on ionic strength and pH.

$$\frac{C_e}{Q_e} = \frac{1}{(bQ_m)} + \frac{1}{(Q_m)} C_e$$

2.8. DRC-ICP-MS analysis

Selenium quantification of the supernatants obtained from the experiments described above was determined by analysis using a Perkin Elmer Elan DRC II ICP-MS with ELAN software. Table 1 describes the operational parameters of the DRC-ICP-MS for selenium analysis. To reduce interferences on the selenium ions during analysis, the samples were ran in dynamic reaction cell (DRC) mode using oxygen gas. The Se-O *m/z* 96 was the chosen ion used for analysis since Se-O production is favored under these conditions. Analysis of selenium was obtained based on calibration curves with a correlation coefficient (r^2) of 0.99 or better.

2.9. Statistical analysis

The obtained data of selenite and selenate binding percentages to both nanomaterials collected from pH, time dependence, and competitive anion studies were analyzed with one-way analysis of variance (ANOVA) using SPSS software, version 12.0 (SPSS, Chicago, IL). The Tukey-HSD (honestly significant difference) test was used to determine significant differences between treatments for each of the aforementioned studies. References to significant differences between treatment means were based on a probability of $p < 0.05$, unless otherwise stated.

3. Results and Discussion

3.1. X-ray diffraction characterization of nanomaterial

Characterization of the non-microwave-assisted and microwave-assisted nanomaterials by XRD revealed that *both* had the crystal structure magnetite (Fe_3O_4). Indeed, as shown by the data in Fig. 1, the XRD patterns exhibit the (220), (311), (400), (422), and (511) Bragg reflections corresponding to the known room temperature phase of magnetite [22]. The other two diffraction peaks present in each pattern are the (111) and (200) reflections from the platinum sample holder. No other peaks are observed, which indicates the impurity-free nature of the Fe_3O_4nanomaterials used in this study. Both synthetic techniques employed here are advantageous due to their simplicity and cost effectiveness compared to other previously reported preparation techniques that involve many steps as well as special chemicals and procedures. Although the two XRD datasets seem very similar upon mere visual inspection, careful Scherrer analysis of the full-width-at-half-maximum (FWHM) carried out on three different peaks in each pattern shows slightly different average grain sizes: 27 +/− 0.48 nm for the non-microwave-assisted and 25 +/− 0.95 nm for the microwave-assisted synthetic nanomaterials. This is *not* insignificant; this difference leads to nanoparticles in the non-microwave-assisted material whose individual volume is ~25%

larger, and whose surface area (for a given sample volume) is ~10% smaller than that of their microwave-assisted counterparts.

3.2. pH binding studies

The sorption of selenite and selenate to both sets of synthetic nanomaterials can be seen in Fig. 2. The binding of selenite to both synthetic Fe_3O_4 nanomaterials was practically pH independent as shown in Fig. 2(A-B). The sorption of selenate had the highest binding at pH 2 to 4 for both synthetic types of Fe_3O_4. A decrease in selenate binding occurred at pH 5 for both particles and a more significant decrease was seen at pH 6. The decrease was higher for the non-microwave assisted synthesized nanomaterial (Fig. 2A), which might be due to the particle size. The decrease in binding could be due to the change in surface charge at higher pH values. It has been reported magnetites have a zero-point charge which mostly occurs in the pH range from 5-7 [23]. When the pH increases the surface of the particle will become less positively charged resulting in a lower binding affinity for anion binding. It has also been shown that selenate has a lower binding affinity to iron oxide surfaces than selenite [24]. Martinez et al. [20] have shown that at pH 6 the sorption of Se(IV) on magnetite is about 20% and the sorption of Se(VI) is about 1%. At pH 8 the sorption of Se(IV) is about 10% while the sorption of Se(VI) is close to 0. This difference in binding affinity between selenite and selenate could be why selenite has a higher binding percentage at pH 6 than that of selenate to both nanomaterials. The lower binding affinity of selenate in addition to the change of surface charge at increasing pH values, could explain the decrease in binding at pH 5 and 6. The remaining experiments were conducted at a pH of 4 for maximum binding of selenate to the nano-magnetite materials. It has also been shown that selenate has a lower binding affinity to iron oxide surfaces than selenite [25].

3.3. Sorption kinetic studies

The binding of selenium oxoanions to non microwave-assisted and microwave-assisted synthetic Fe_3O_4 nanomaterials as a function of time is shown in Fig. 3(A-B). Statistical analysis with one-way ANOVA determined that there was no significant difference in the binding of selenite or selenate to either non-microwave-assisted Fig. 3A) or microwave-assisted (Fig. 3B) synthetic Fe_3O_4 in a time range of 5 to 60 min. Su and Suarez [26] have shown that selenite and selenate binding equilibrates within 25 min of contact time to iron oxides and goethitite. It is interesting to note the rapid binding of selenite to synthetic Fe_3O_4 with average particle size of 4 nm within 10 min of contact time has been shown by Lopez de Arroyabe Loyo *et al.* [21]. Martinez *et al.* [20] reported that both selenite and selenate binding to a natural magnetite with a particle size <5 μm took over 24 h to reach maximum binding capacity. This observation suggests that even though the synthetically produced nanomaterials used in this study are almost 7 times larger than those produced and used by Lopez de Arroyabe Loyo *et al.* [21], the fact these particles are at nanoscale produces faster binding times than micrometer sized particles. The Fe_3O_4 nanomaterial is non-porous so the smaller the particle, the larger surface area with more available binding sites for selenium oxoanion binding to occur. This suggests the binding is occurring on the surface without the occurrence of a redox reaction. This would indicate the oxidation states of both selenite and selenate will remain the same. Our XAS results (not shown) corroborated previous report by Lopez de Arroyabe Loyo *et al.* [21] that have shown by extended X-ray absorption fine

structure (EXAFS) no shift of backscattering contribution in the coordination shell of Se and Fe between 2.3 to 2.6 Å.

3.4. Competitive anion studies

The results of the competition study on selenite and selenate to both non microwave-assisted and microwave-assisted synthesized nanomaterials in the presence of varying concentrations of Cl^-, NO_3^-, SO_4^{2-}, or PO_4^{3-} added can be seen in Fig. 4-7. As shown in Fig. 4(A-B), the addition of Cl^- at concentrations varying from 0.1 to 100 ppm had no significant effect on the percentage of both selenite and selenate binding to either Fe_3O_4 nanomaterial. This indicates the Cl^- ion has a low binding affinity for Fe_3O_4. A similar observation of Cl^- not acting as a competitive anion for the iron oxide surface was reported by Jeong *et al.* [27]. These similarities in results indicate that chloride has a low binding affinity for iron oxide surface and complexes formed between chloride and iron oxide surface are weaker than those between iron oxide and selenium.

While the addition of NO_3^- did not have an effect on selenate binding to the non microwave-assisted synthetic Fe_3O_4 (Fig. 5A), the anion did lower selenate binding by 30% on the microwave-assisted synthetic Fe_3O_4 material. However, the inclusion of NO_3^- did not affect the binding of selenite to either of the two synthetically different Fe_3O_4 as can be seen in Fig. 5(B). This non-competitive effect of the nitrite anion could be behaving the same as the chloride anion. One possible explanation for the decrease in selenate binding to only the microwave-assisted synthetic Fe_3O_4 material is the size of the material. Dhillon and Dhillon [28] have stated that competitive effect of sorbed anions could occur either by physical competition for binding sites or through electrostatic competition results from a change in electrostatic potential. As explained in the X-ray diffraction analysis of the two different synthetically produced nanomaterials, the microwave-assisted synthetic technique resulted in a smaller average particle size of Fe_3O_4 than that of the non microwave-assisted synthetic technique. A smaller particle size would result in larger surface area and a higher number of binding sites. This greater number of binding sites along with selenate having a lower binding affinity than observed for selenite could allow the NO_3^- to compete to a higher extent with the selenate oxoanion present in solution.

The effects of the addition of SO_4^{2-} on selenite or selenate binding to the two synthetic nanomaterials can be seen in Fig. 6. Selenite did not experience a significant decrease in binding in the presence of SO_4^{2-}in a range of 0.1-100 ppm which is shown in Fig. 6B. Goh and Lim [29] and Zhang *et al.* [30] have shown similar results with selenite binding being hardly affected by addition of SO_4^{2-}oxoanion to iron oxide containing tropical sand and iron-coated granular activated carbons (GAC), respectively. There was a decrease of selenate binding to both microwave-assisted and non microwave-assisted synthesized nanomaterials beginning at 1 and 10 ppm, respectively. In the presence of 1 ppm sulfate, the molar ratio of selenate to sulfate is 1 SeO_4^{2-} : 14.9 SO_4^{2-}. The non microwave-assisted material still had around 100 % binding while the microwave assisted material had 60% binding. This indicates both Fe_3O_4 materials have a high affinity for selenate. The differences in binding percentages between the microwave-assisted and non microwave-assisted materials are occurring due to the differences in surface area generated by the two

synthetic techniques. At 10 ppm of sulfate present, the molar ratio of selenate to sulfate is 1 SeO_4^{2-} : 149 SO_4^{2-}. Again, at these ratios selenate binding decreased for both Fe_3O_4 particles to 15 and 80% binding for non microwave-assisted and microwave-assisted synthetic Fe_3O_4, respectively. When in the presence of 100 ppm sulfate the molar ratio of selenate to sulfate was SeO_4^{2-}: 1488 SO_4^{2-}. Even though the binding percentages are 6% and 20% for non microwave-assisted and microwave-assisted nanomaterials, respectively, binding occurring at this molar ratio is still indicative of the affinity for selenate to Fe_3O_4 materials. It is known the chemistry of selenate and sulfate is quite similar. This similarity in chemistry could be the explanation of the decreased sorption of selenate in the presence of sulfate. Zhang *et al.* [30] described this effect by explaining both anions tend to form weak bonds with surface sites which could be more easily released. The smaller particle size of the microwave-assisted synthesized Fe_3O_4, as described above, could explain why binding started to decrease at a lower concentration of SO_4^{2-}(1 ppm) as opposed to the non microwave-assisted synthetic Fe_3O_4 binding (10 ppm).

The competitive effect of the addition of PO_4^{3-} anion on selenite and selenate binding to both synthetic Fe_3O_4 nanomaterials can be seen in Fig. 7. The addition of PO_4^{3-} had a greater affect on the binding of selenate to the synthetic Fe_3O_4 nanomaterials than any other anion investigated in this study. A decrease in selenite binding to microwave-assisted and non microwave-assisted synthetic Fe_3O_4 nanomaterials was observed to begin at the introduction of 10 and 100 ppm of PO_4^{3-} respectively. In the presence of 100 ppm PO_4^{3-}, the molar ratio of selenite to phosphate is 1 SeO_3^{2-}: 1000 PO_4^{3-}. Even at this large molar ratio of sulfate to selenite ions present, there is still selenite binding occurring to the non microwave-assisted synthetic material. This would indicate the effect was due to the difference in molar ratios and competitive effect rather than that of a mono, bi, or tri-anion effect. In addition, the phosphate ion has an additional oxygen, therefore the selenite affinity and size make it easier for it to bind and take up less space on the surface of the material.

A decrease in binding of selenate to microwave-assisted synthetic Fe_3O_4 was observed to occur not only with a lower concentration of PO_4^{3-} introduced, but at a greater extent than that of the non microwave-assisted synthetic Fe_3O_4 nanomaterial. These trends have been observed by Goh and Lim [29] and Zhang *et al.* [30] in tropical sand containing iron oxides and iron-coated GAC, respectively. As explained previously, the differences in the selenium binding percentages between the non microwave-assisted and microwave-assisted nanomaterials could be a result of the smaller particle size of the microwave-assisted synthetic Fe_3O_4 nanomaterial. A significant decrease of less than 1% and 0% selenate binding to non microwave-assisted synthetic and microwave-assisted synthetic Fe_3O_4, respectively was observed to occur at the addition of 100 ppm of PO_4^{3-}. The inclusion of 100 ppm PO_4^{3-} in solution results in a molar ratio of 1 SeO_4^{2-} : 1505 PO_4^{3-}. There had to be 1505 times the concentration of phosphate present to for selenate binding to decrease to almost 0%. It has been described in the literature that the PO_4^{3-} $_4$oxoanion is very adsorptive to the surfaces of iron oxides in low concentration range [27].

3.5. Adsorption isotherms

The binding capacities of both the non microwave-assisted and microwave-assisted synthesized Fe_3O_4 nanomaterials were based on the fitting of selenite and selenate sorption studies to Langmuir isotherms equation as seen in Figures 8 and 9. The capacities as a result of the fitting are detailed in Table 2. The non microwave-assisted synthesized Fe_3O_4 nanomaterial had a capacity of 1923 and 1428 mg Se/kg of Fe_3O_4 for selenite and selenate, respectively. The microwave-assisted synthetic nanomaterial was determined to have a higher capacity for both selenite and selenate of 2380 and 2369 mg Se/kg of Fe_3O_4, respectively than that of the non-microwave assisted nanomaterial. The higher capacity of the microwave-assisted material could be the result of its smaller size than that of the non microwave-assisted synthetic material. The average grain size of the microwave assisted nanoparticles was approximately 25 nm and that of the open vessel was 27 nm; this would account for the small sorption observed in the capacities (approximately 7-8 % difference in the diameter which results in approximately a 20% difference in the surface area of the particles).

As explained earlier, the smaller particle would result in a greater number of surface sites for selenium oxoanion binding to occur. This increase would allow for a higher capacity of the nanomaterial. Goh and Lim [29] reported 145 mg Se/ kg of tropical soil for selenite removal which is a much lower adsorption value for selenite than the synthetic magnetite produced in this study. Naturally occurring magnetite was also observed to have lower capacities for both selenite and selenate of 352.95 and 484.63 mg Se/ kg of magnetite [20]. This observation in the differences in capacities of naturally occurring and the synthetic magnetite prepared for these studies could be explained by the size differences of the magnetite as stated previously. The reported capacities of selenite and selenate to iron-coated GAC adsorbents at room temperature were 637 and 220 mg Se/ g of Fe-GAC, respectively were also lower than the capacities reported in this study [30-31].

4. Conclusions

The results of this work show that both non-microwave assisted and microwave-assisted synthesized Fe_3O_4 are capable of binding both selenite and selenate oxoanions. The binding of both oxoanions to the nanomaterial had an optimum pH of 4 and reached equilibrium within 5 min of contact time. These results are consistent with the anion binding to materials with similar surface properties. The anions SO_4^{2-} and PO_4^{3-} affected the binding of both oxoanions to the greatest extent. The non microwave-assisted synthesized Fe_3O_4 nanomaterial had a capacity of 1923 and 1428 mg Se/kg of Fe_3O_4 for selenite and selenate, respectively. The microwave-assisted synthetic material was determined to have a higher capacity for both selenite and selenate of 2380 and 2369 mg/kg of Fe_3O_4, respectively than that of the non microwave-assisted material. These results suggest that both synthetic materials can be used to remove selenium from contaminated waters. Also, synthetic methods used in this study require less steps, special chemicals, and procedures than previously reported preparation techniques. Additionally, the removal time and capacities of both Se(IV) and Se(VI) using both synthetic materials tested were faster and higher than previous materials tested. However, the materials and technique investigated in this study

would experience limitations in the presence of competitive anions. Further studies would need to be performed to determine efficiency of these materials in a larger system for the remediation of Se(IV) and Se(VI) from contaminated water.

Acknowledgements

This material is based upon work supported by the National Science Foundation and the Environmental Protection Agency under Cooperative Agreement Number DBI-0830117. Any opinions, findings, and conclusions or recommendations expressed in this material are those of the author(s) and do not necessarily reflect the views of the National Science Foundation or the Environmental Protection Agency. This work has not been subjected to EPA review and no official endorsement should be inferred. The authors also acknowledge the USDA grant number 2008-38422-19138, the Toxicology Unit of the BBRC (NIH NCRR Grant # 2G12RR008124-16A1), and the NSF Grant # CHE-0840525. J. L. Gardea-Torresdey acknowledges the Dudley family for the Endowed Research Professorship in Chemistry. C.M. Gonzalez acknowledges the NSF Graduate Teaching Fellows in K-12 Education (DGE#0538623).

References

1. Pinochet H, de Gregori I, Lobos MG, Fuentes E. Selenium and copper in vegetables and fruits grown on long-term impacted soils from Valparaiso region, Chile. Bull. Environ. Contam. Toxicol. 1999; 63:327–334. [PubMed: 10475910]
2. United States Environmental Protection Agency (USEPA). Edition of the drinking water standards and health advisories, EPA-822-R-06-013, Office of Water. USEPA; Washington, DC.: 2006.
3. Mandal S, Mayadevi S, Kulkarni BD. Adsorption of Aqueous Selenite [Se(IV)] Species on Synthetic Layered Double Hydroxide Materials. Ind. Eng. Chem. Res. 2009; 48:7893–7898.
4. Hoffman DJ. Role of Selenium toxicity and oxidative stress in aquatic birds. Aquat. Toxicol. 2002; 57:11–26. [PubMed: 11879935]
5. Strawn D, Doner H, Zavarin M, McHugo S. Microscale investigation into the geochemistry of arsenic, selenium, and iron in soil developed in pyritic shale materials. Geoderma. 2002; 108:237–257.
6. Frankenberger WT, Arshad M. Bioremediation of selenium-contaminated sediments and water. BioFactors. 2001; 14:241–254. [PubMed: 11568461]
7. Marvo V, Stamenov S, Todorova E, Chimel H, Erwe T. New hybrid electro-coagulation membrane process for removing selenium from industrial wastewater. Desalination. 2006; 201:290–296.
8. El-Shafey EI. Removal of Se(IV) from aqueous solution using sulphuric acid-treated peanut shell. Journal of Environmental Management. 2007; 84:620–627. [PubMed: 17493740]
9. Zhang M, Reardon EJ. Removal of B, Cr, Mo, and Se from Wastewater by Incorporation into Hydrocalumite and Ettringite. Environ. Sci. Technol. 2003; 37:2947–2952. [PubMed: 12875399]
10. Roussel T, Bichara C, Pellenq RJM. Selenium and carobon nanostructures in the pores of $AlPO_4$-5. Adsorption. 2005; 11:709–714.
11. Sabarudin A, Oshita K, Oshima M, Motomizu S. Synthesis of chitosan resin possessing 3,4-diamino benzoic acid moiety for the collection/concentration of arsenic and selenium in water samples and their measurement by inductively coupled plasma-mass spectrometry. Anal. Chim. Acta. 2005; 542:207–215.
12. Ippolito JA, Scheckel KG, Barbarick KA. Selenium adsorption to aluminum-based water treatment residuals. J. Colloid Interface Sci. 2009; 338:48–55. [PubMed: 19589535]
13. Bonhoure I, Baur I, Wieland E, Johnson CA. Uptake of Se(IV/VI) oxyanions by hardened cement paste and cement minerals: An X-ray absorption spectroscopy study. Cem. Concr. Res. 2006; 36:91–98.
14. Peak D. Adsorption mechanisms of selenium oxyanions at the aluminum oxide/water interface. J. Colloid Interface Sci. 2006; 303:337–345. [PubMed: 16949599]
15. Parida KM, Gorai B, Das NN, Rao SB. Studies on ferric oxide hydroxides: Adsorption of selenite (SeO_3^{2-}) on different forms of iron oxyhydroxides. J. Colloid Interface Sci. 1997; 185:355–362. [PubMed: 9028889]

16. Lo SL, Chen TY. Adsorption of Se(IV) and Se(VI) on an iron-coated sand from water. Chemosphere. 1997; 35:919–930.

17. Zhang Y, Wang J, Amrhein C, Frankenberger WT. Removal of selenate from water by zerovalent iron. J. Environ. Qual. 2005; 34:487–495. [PubMed: 15758101]

18. Oliveira LCA, Rios VRA, Fabris JD, Sapag K, Garg VK, Lago RM. Clay-oxide magnetic composites for the adsorption of contaminants in water. Appl. Clay Sci. 2003; 22:169–177.

19. Rocher V, Siaugue J, Cabuil V, Bee A. Removal of organic dyes by magnetic alginate beads. Water Res. 2008; 42:1290–1298. [PubMed: 17980401]

20. Martinez M, Gimenez J, de Pablo J, Rovira M, Duro L. Sorption of selenium (IV) and selenium (VI) onto magnetite. Appl. Surf. Sci. 2006; 252:3767–3773.

21. Lopez de Arroyabe Loyo R, Nikitenko SI, Scheinost AC, Simonoff M. Immobilization of selenite on Fe_3O_4 and Fe/Fe_3C Ultrasmall particles. Environ. Sci. Technol. 2008; 42:2451–2456. [PubMed: 18504980]

22. Sreeja V, Joy PA. Microwave–hydrothermal synthesis of γ-Fe_2O_3 nanoparticles and their magnetic properties. Mater. Res. Bull. 2007; 42:1570–1576.

23. Kosmulski, M. Surfactant Science Series. Vol. 145. Taylor & Francis Group; Bocan Rayon, FL: 2009. Surface Charging and Points of Zero Charge; p. 222-233.

24. Manceau A, Charlet L. The mechanism of selenate adsorption on goethite and hydrous ferric oxide. J. Colloid Interface Sci. 1994; 168:87–93.

25. Parsons JG, Lopez ML, Peralta-Videa JR, Gardea-Torresdey JL. Determination of arsenic (III) and arsenic (V) binding to microwave assisted hydrothermal synthetically prepared Fe_3O_4, Mn_3O_4, and $MnFe_2O_4$ nanoadsorbents. Microchem. J. 2009; 91:100–106.

26. Su C, Suarez DL. Selenate and Selenite Sorption on Iron Oxides: An Infrared and Electrophoretic Study. Soil Sci. Soc. Am. J. 2000; 64:101–111.

27. Jeong Y, Maohong F, Van Leeuwen J, Belczyk JF. Effect of competing solutes on arsenic(V) adsorption using iron and aluminum oxides. J. Environ. Qual. 2005; 34:487–495. [PubMed: 15758101]

28. Dhillon SK, Dhillon KS. Selenium adsorption in soils as influenced by different anions. J. Plant Nutr. Soil Sci. 2000; 163:577–582.

29. Goh K, Lim T. Geochemistry of inorganic arsenic and selenium in a tropical soil: effect of reaction time, pH, and competitive anions on arsenic and selenium adsorption. Chemosphere. 2004:849–859. [PubMed: 15041289]

30. Zhang N, Lin L, Gang D. Adsorptive selenite removal from water using iron-coated GAC adsorbents. Water Res. 2008; 42:3809–3816. [PubMed: 18694584]

31. Zhang N, Gang D, Lin L. Adsorptive removal of ppm-level selenate using iron-coated GAC adsorbents. J. of Environ. Eng. 2010; 136:1089–1095.

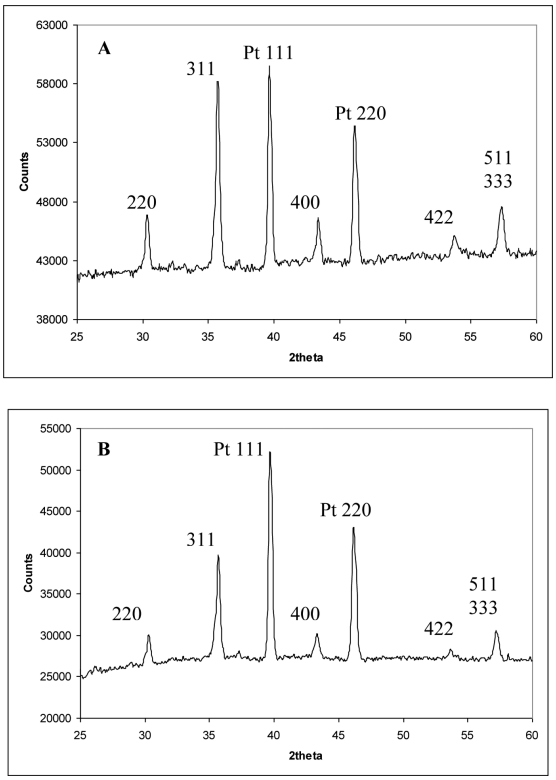

Fig. 1.

X-ray diffraction pattern of Fe_3O_4 from titration of iron(II) chloride with sodium hydroxide. (A) non microwave-assisted synthesis. (B) microwave-assisted synthesis.

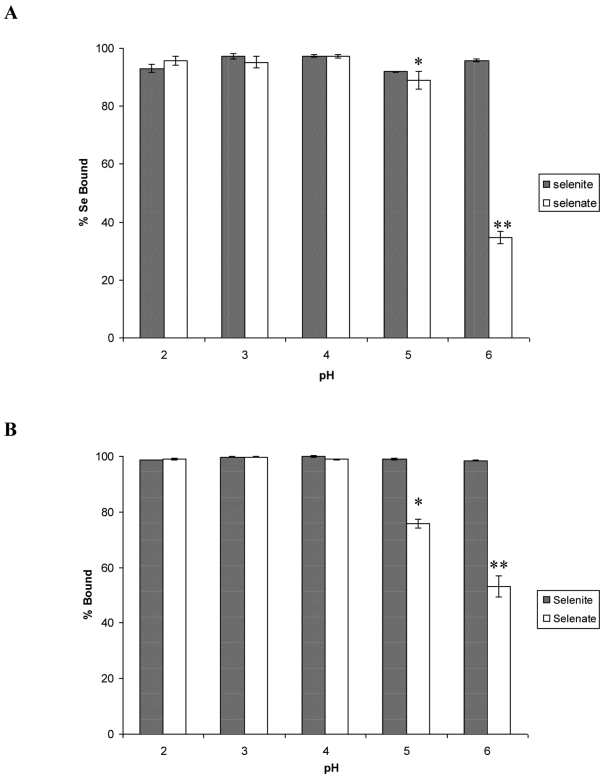

Fig. 2.

Percentage bound of selenite and selenate at a concentration of 100 ppb to the nanomaterial under varying pH conditions ranging from pH 2 to 6. (A) non microwave-assisted Fe_3O_4. (B) microwave-assisted Fe_3O_4. Error bars represent Standard Error of three replicate. * represents statistical differences at $p \leq 0.05$.

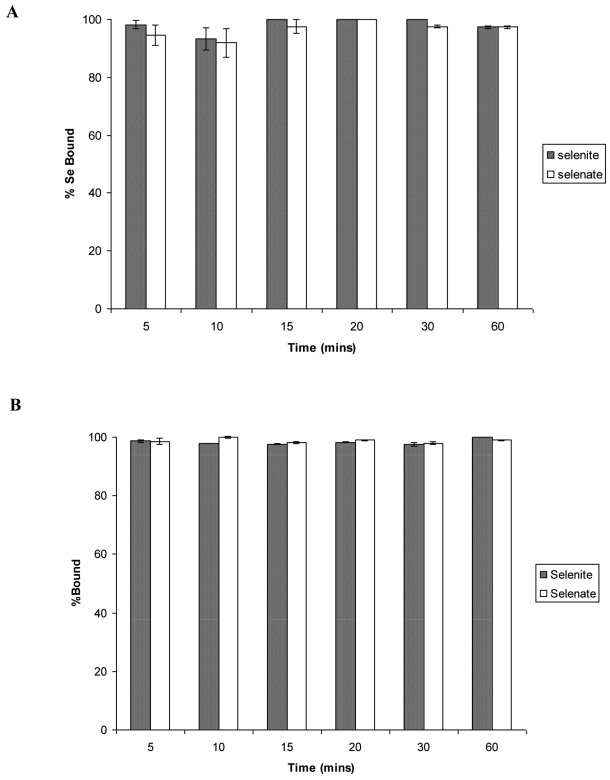

Fig. 3.

Time dependence of percentage bound of selenite and selenate to the nanomaterial at a pH of 4. (A) non microwave-assisted Fe_3O_4. (B) microwave-assisted Fe_3O_4. Error bars represent Standard Error of three replicate.

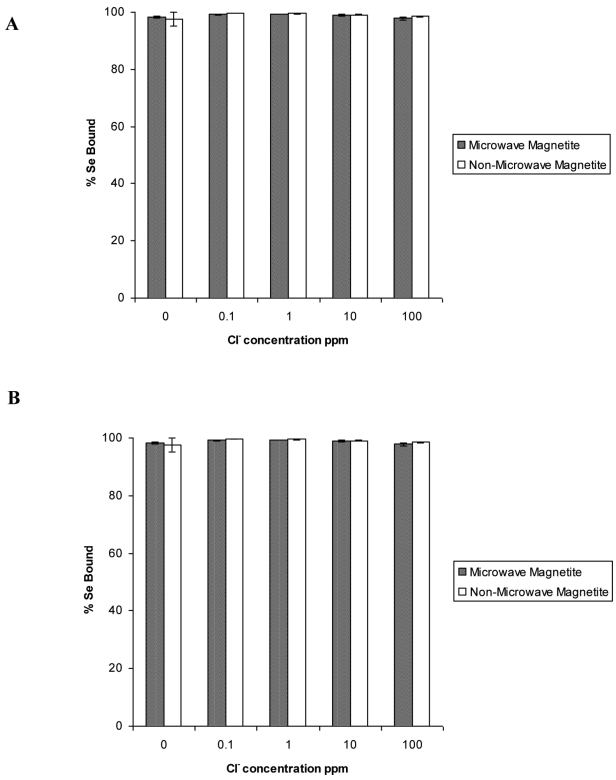

Fig. 4.

The effects of the Cl^- ion ranging in concentration from 0.1-100 ppm on the sorption of selenite and selenate to non microwave-assisted and microwave-assisted Fe_3O_4. (A) Selenate.

(B) Selenite. Error bars represent Standard Error of three replicate.

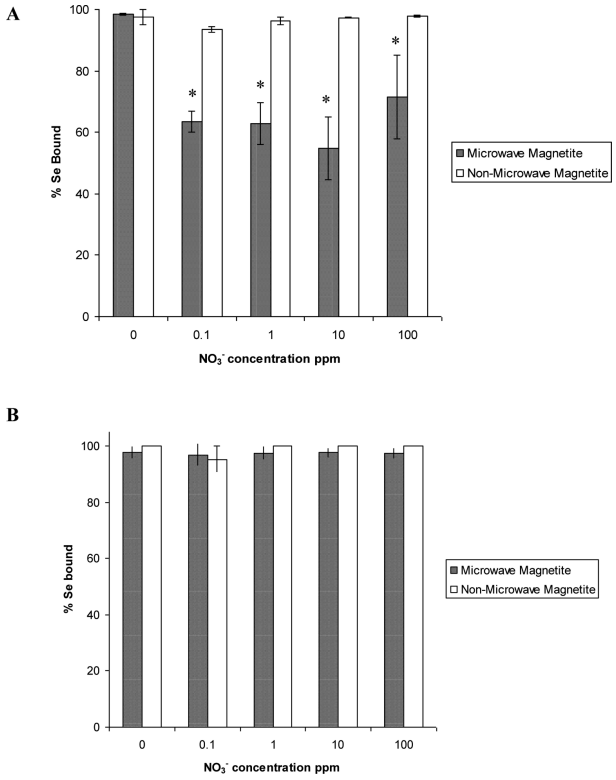

Fig. 5.

The effects of the NO_3^- ion ranging in concentration from 0.1-100 ppm on the sorption of selenite and selenate to non microwave-assisted and microwave-assisted Fe_3O_4. (A) Selenate. (B) Selenite. Error bars represent Standard Error of three replicate. * represents statistical differences at $p \leq 0.05$.

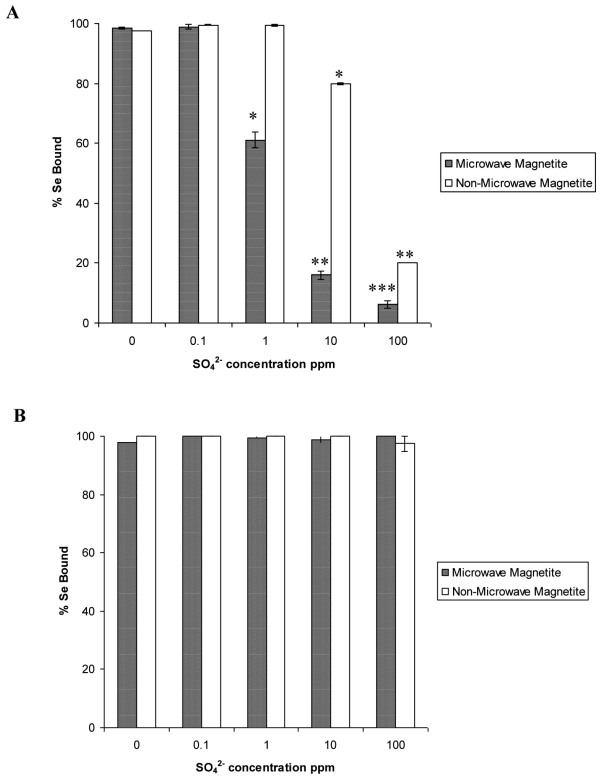

Fig. 6.

The effects of the SO_4^{2-} ion ranging in concentration from 0.1-100 ppm on the sorption of selenite and selenate to non microwave-assisted and microwave-assisted Fe_3O_4. (A) Selenate. (B) Selenite. Error bars represent Standard Error of three replicate. * represents statistical differences at $p \leq 0.05$.

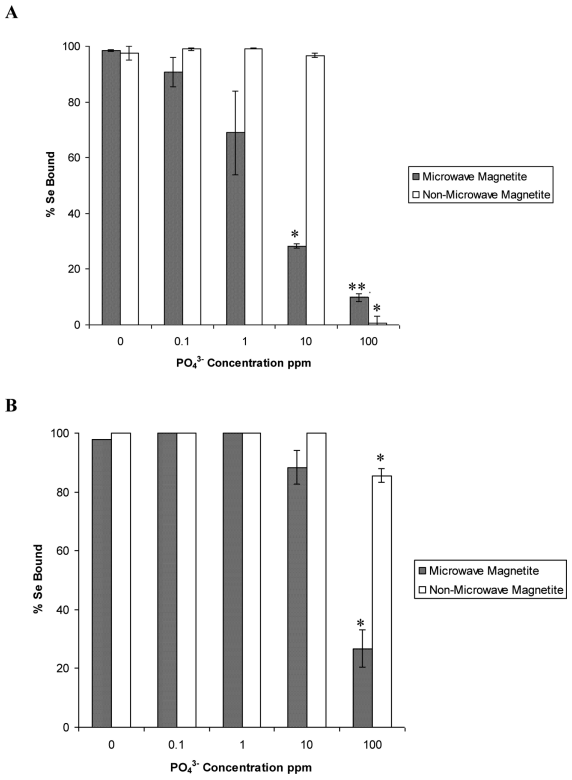

Fig. 7.

The effects of the PO_4^{3-} ion ranging in concentration from 0.1-100 ppm on the sorption of selenite and selenate to non microwave-assisted and microwave-assisted Fe_3O_4. (A) Selenate.

(B) Selenite. Error bars represent Standard Error of three replicate. * represents statistical differences at $p \leq 0.05$.

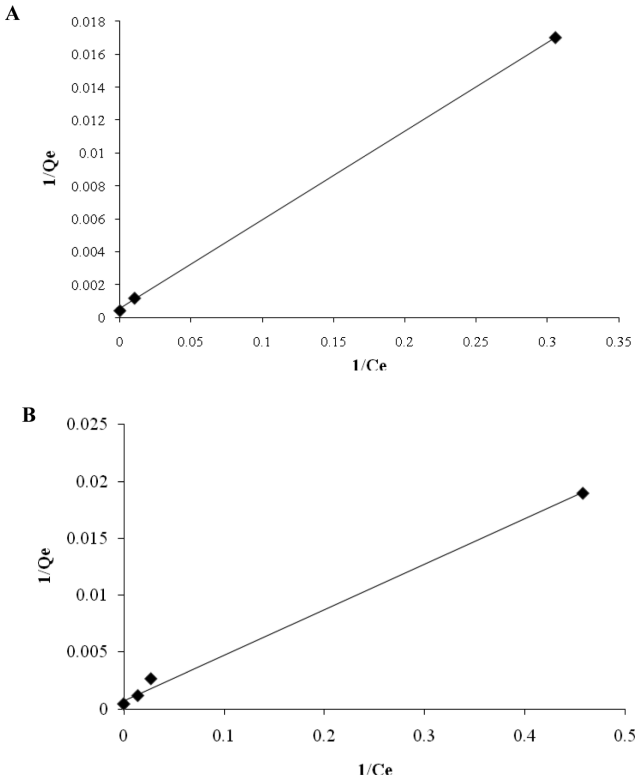

Fig. 8.

The Langmuir isotherm fittings of both selenite and selenate binding onto non microwave-assisted Fe_3O_4 nanomaterial. (A) Selenite. (B) Selenate.

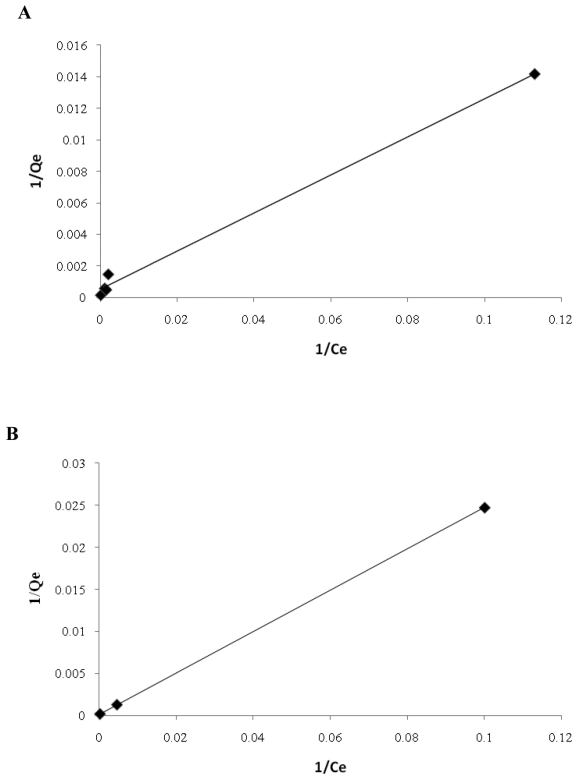

Fig. 9.

The Langmuir isotherm fittings for both selenite and selenate binding onto microwave-assisted Fe_3O_4 nanomaterial. (A) Selenite. (B) Selenate.

Table 1

ICP-MS settings used for the determination of Se concentration in collected supernatants upon reaction with either non microwave-assisted or microwave-assisted synthesized nanomaterial.

Parameter	Setting
RF Power	1200W
Nebulizer	Meinhard Type A Quartz
Nebulizer flow	0.95 L/min
Spray chamber	Glass cyclonic
Injector	Quartz
Plasma flow (Ar)	15 L/min
CeO/Ce	<5%
Ba^{+}/Ba^{++}	<5%
O_2	0.85 mL/min

Table 2

Capacities based on Langmuir isotherm experiments for both selenite and selenate binding to non microwave-assisted and microwave-assisted Fe_3O_4 nanomaterials.

Nanomaterial	Adsorbate	Q_e (mg Se/kg of Fe_3O_4)	R^2
Non microwave-assisted Fe_3O_4	SeO_3^{2-}	1923±119.877	1.0
	SeO_4^{2-}	1428±71.4	0.997
Microwave-assisted Fe_3O_4	SeO_3^{2-}	2380±7.14	0.990
	SeO_4^{2}	2369±16.58	1.0